Hydrodynamics of Nanoscopic Tubulin Rings in Dilute Solutions

Hacène Boukari,[1,*] Ralph Nossal,[1] Dan L. Sackett,[1] and P. Schuck[2]
[1]*Laboratory of Integrative and Medical Biophysics, NICHD, Bethesda, Maryland 20892, USA*
[2]*Division of Bioengineering and Physical Science, ORS/OD, National Institutes of Health, Bethesda, Maryland 20892, USA*
(Received 28 January 2004; published 26 August 2004)

We combine fluorescence correlation spectroscopy and sedimentation velocity measurements to probe the hydrodynamic behavior of tubulin dimers and nanoscopic tubulin rings. The rings are rigid, have circular geometry, and are monodisperse in size. We use the high-precision ratio of the sedimentation coefficients and that of the translational diffusion coefficients to validate theories for calculating the hydrodynamic properties of supramolecular structures.

DOI: 10.1103/PhysRevLett.93.098106 PACS numbers: 87.15.–v, 87.64.–t, 87.68.+z

Various biological entities have a well-defined toroidal, or ringlike, shape when in aqueous solution. Examples are bacteriophage DNA condensed with multivalent cations [1,2], hexameric protein complexes involved in DNA replication [3,4], assemblies of RNA binding proteins [5], tubulin-containing ring structures [6–8], and dynamin oligomers [9]. In this Letter we focus on nanoscopic protein ring polymers that form when $\alpha\beta$-tubulin dimers ("Tu"−MW∼100 kDa) bind cryptophycin molecules ("Cr" − MW ∼ 350 Da). These tubulin ring polymers have several attributes that can be exploited for testing the validity of hydrodynamic theories of supramolecular structures: namely, well-defined circular geometry, very narrow dispersity in structure, high rigidity, and good stability against dilution [6,7,10,11]. Crucial to this study is the finite number of the subunits (tubulin) that composes the closed ring polymers, unlike the open-ended supramolecular structures such as microtubules and actin filaments.

We combine measurements of these rings and their protein subunits, obtained by two independent techniques: fluorescence correlation spectroscopy (FCS) [10,12–15] and sedimentation velocity analytical ultracentrifugation (SV) [16]. We show precise quantitative agreement between the ratios of the diffusion coefficients of these supramolecules and those of their sedimentation coefficients. More importantly, we make use of the precision of the ratios to test the applicability of theoretical analyses that relate the structure of nanoscopic objects of complex shape to their hydrodynamic properties.

The $\alpha\beta$-tubulin dimer, which is the basic building block of tubulin polymers, is a protein composed of two subunits differing in sequence but having very similar shape (width: 4.6 nm; height: 4.0 nm; depth: 6.5 nm) and molecular weight [17]. Tubulin is ubiquitously found in eukaryotic cells and is the principal constituent of microtubules, which are primary components of several critically important cytoskeletal structures [18]. However, cryptophycin, a cyclic depsipeptide obtained from cyanobacteria [7], causes significant depolymerization of microtubules and induces, instead, the formation of closed rings (∼ 24.8 nm diameter [6,10]). The rings contain eight tubulin dimers (see Fig. 1 inset) and, for the solution conditions in this investigation, only individual tubulin dimers and closed rings seem to be present.

FCS and SV measurements yield, respectively, the distributions of the hydrodynamic diameters and sedimentation coefficients of the polymeric structures in the cryptophycin-tubulin solutions. These can be compared

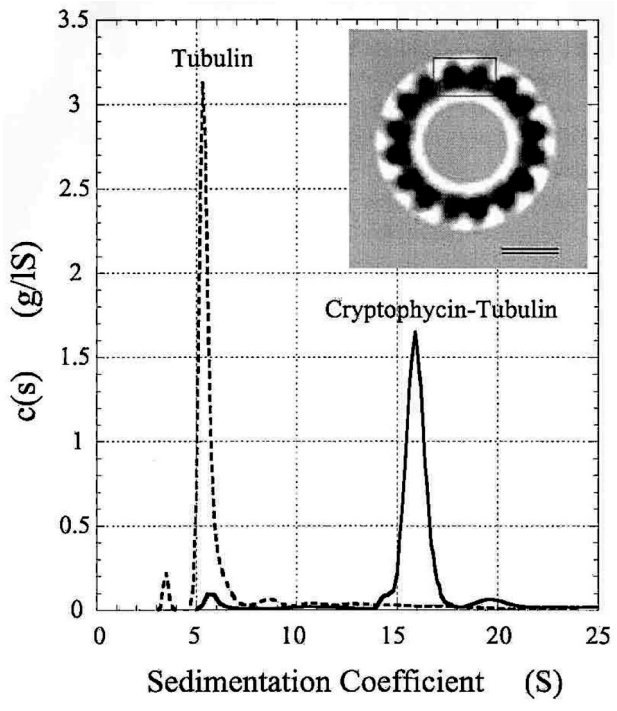

FIG. 1. Distributions of the sedimentation coefficients determined by inversion of SV centrifugation profiles measured on tubulin and tubulin-cryptophycin solutions at 25 000 rpm and 50 000 rpm, respectively, (Svedberg = 10^{-13} sec). Inset shows an averaged image of cryptophycin-tubulin rings from cryo-electron microscopy [6]. The box encloses one tubulin dimer and the bar represents 10 nm.

with those of the primary tubulin solutions (no cryptophycin). For analysis we use the Svedberg equation [19] and derive a simple expression that relates the ratio of the hydrodynamic diameters of the tubulin dimers and the tubulin rings to the corresponding ratio of sedimentation rates. Various experimental parameters such as solvent viscosity, temperature, partial specific volume, and monomer mass do not appear in this expression, enabling a direct comparison with ratios calculated from different structural models.

Cow brain tubulin, both unlabeled and fluorescently labeled with an average of one tetramethylrhodamine fluorophore per tubulin dimer, was acquired from Molecular Probes (Eugene, OR) and used without further purification. Cryptophycin 1 was obtained from the Cancer Research Center of Hawaii. For FCS measurements, the cryptophycin-tubulin samples (CrTu) were prepared by mixing $[\mathrm{Tu}] = 5\ \mu\mathrm{M}$ and $[\mathrm{Cr}] = 8\ \mu\mathrm{M}$ in PIPES buffer (0.1 M PIPES (Piperazine-N, N′-bis-(2-ethanesulfonic acid), $[\mathrm{MgCl_2}] = 1$ mM, pH 7.0) and then diluting to concentration $\simeq 100$ nM. SV experiments require relatively high concentrations of tubulin ($[\mathrm{Tu}]=3\ \mu\mathrm{M}$, $[\mathrm{Cr}] = 5\ \mu\mathrm{M}$ in 0.1 M MES (2-(N-Morpholino) ethanesulfonic acid) buffer pH 6.9, $[\mathrm{MgCl_2}] = 1$ mM). All measurements were performed at room temperature.

SV data were collected at two different rotor speeds (25 000 rpm and 50 000 rpm) with an Optima XL-I/A analytical ultracentrifuge (Beckman Coulter, Fullerton, CA). For each sample, a 400 microliter aliquot was placed in the sample sector of an Epon double-sector centerpiece, and the same volume buffer or buffer containing 5 μM Cr was placed in the reference sector. The differential refractive index distribution across the solution column was measured at 60 s time intervals using laser interferometry imaging and profiles were then analyzed with the Lamm equation as described in [16,20]. Here we applied, in two steps, the software SEDPHAT [21] to invert the profiles into distributions, $c(s)$, of the sedimentation coefficients, s, of the various sedimenting components in the solutions.

We first considered the $c(s)$ distribution to be continuous, and fitted the measured profiles using algebraic decomposition of the systematic time-invariant fringe shifts [20] and maximum entropy regularization that yields the least-biased distribution [16]. Figure 1 shows a pronounced peak at $s \simeq 5.5$ in the $c(s)$-distribution for the Tu sample and, in contrast, a pronounced peak at $s \simeq 15.9$ in that for the CrTu sample, which can be ascribed to 8-dimer rings. In the CrTu distribution, there is also a small peak compatible with the major peak of the Tu sample, indicating the presence of a small amount of unpolymerized tubulin. Another relatively broad but small peak can be discerned in the CrTu sample at $s \simeq 19$, which may be attributed to aggregates of tubulin rings or other unknown assemblies of tubulin. More interestingly, Fig. 1 indicates that there are no substantial amounts of stable oligomers intermediate between the dimers and the 8-dimer rings in the CrTu sample.

The widths of the dimer and ring peaks in Fig. 1 are misleading in that they suggest relatively large structural heterogeneity in both the tubulin dimer and the ring, contrary to what is known about the system. That is, tubulin has a well-defined, stable structure under the studied conditions, here validated by the high degree of polymerization of tubulin into rings. The widths are artifacts of the maximum entropy regularization used to prevent numerical instabilities in the inversion. So, in the second step, we fitted the profiles with a hybrid piecewise sum of *discrete and continuous* distributions, replacing the peak regions of the $c(s)$-distributions in Fig. 1 with Dirac δ-functions representing individual, single sedimenting components for tubulin dimers and complete 8-dimer rings. The rest of unidentified components were described by a continuous background function. Further, we used the Svedberg equation [19]:

$$s = \frac{MD(1 - \bar{v}\rho)}{RT}, \tag{1}$$

which relates the translational diffusion coefficient D, the molar mass M, and the sedimentation coefficient. In Eq. (1), $\bar{v}$ is the partial specific volume, ρ the density of the solvent, and R the gas constant. The ratio of molar mass of the ring to that of the dimer was set to 8, resulting in three fitting parameters [s(Tu), D(Tu), and $\sigma = s(\mathrm{ring})/s(\mathrm{Tu})$]. These parameters were determined by nonlinear least-squares fitting of four sets of SV data (270 000 points) obtained from the Tu and CrTu samples. We extracted a refined ratio, $\sigma = s(\mathrm{ring})/s(\mathrm{Tu}) = 2.89 \pm 0.02$, where rms errors are comparable to the noise of the data acquisition.

For FCS measurements, fluorescence intensities, $I(t)$, were acquired for short intervals of time Δt at times t, and time correlated to generate a correlation function [14],

$$G(\tau) = 1 + \frac{\langle \delta I(t) \delta I(t + \tau) \rangle}{\langle I(t) \rangle^2}. \tag{2}$$

Here, $\delta I(t) = I(t) - \langle I(t) \rangle$ denotes the spontaneous deviations of the measured intensity from the average intensity, $\langle I(t) \rangle$, and τ is the delay time. For noninteracting fluorescent particles diffusing freely in a Gaussian beam, Eq. (2) becomes [13,15]

$$G(\tau) = 1 + \frac{1}{[\sum_j N_j Q_j]^2} \sum_i \frac{N_i Q_i^2}{(1 + \frac{\tau}{\tau_{di}})(1 + p\frac{\tau}{\tau_{di}})^{0.5}}, \tag{3}$$

where N_i denotes the average number of the fluorescent particles of the i^{th} species and Q_i the fluorescence quantum yield per particle. The Gaussian beam, $W(r, z) = Ae^{-2(r/r_o)^2} e^{-2(z/z_o)^2}$, is characterized by two length scales,

r_o and z_o, defined in the focusing plane and the optical axis along the direction of the beam, respectively. In Eq. (3), $p = (r_o/z_o)^2$ is an instrumental constant and $\tau_{di} = (r_o)^2/4D_i$, D_i being the diffusion coefficient of the i^{th} species. An equivalent description of D_i is the apparent hydrodynamic diameter d_{Hi} defined by the Stokes-Einstein relation $D_i = k_B T/3\pi\eta d_{Hi}$. Here k_B, T, and η are the Boltzmann constant, the temperature of the sample, and the viscosity of the solvent.

FCS data were collected as described elsewhere [10]. In Fig. 2 we show FCS functions of the Tu ([Tu]=100 nM) and CrTu ([Tu]=120 nM, [Cr]/[Tu] = 1.6) samples collected over a 10 to 20 min time period. Two aspects of the curves indicate polymerization of the tubulin into closed rings. First, compare the amplitude $G(\tau \to 0)$ of both FCS curves and identify the limiting values, $N_{\text{app}} = 1/[G(\tau \to 0) - 1]$, the apparent numbers of particles. After accounting for the difference in tubulin concentration between the two samples, we determine the ratio $N_{\text{app}}(\text{Tu})/\text{N}_{\text{app}}(\text{CrTu}) = 5.0$ which, however, should be 8 if the tubulin dimers are labeled uniformly and all polymerize into rings. This apparent discrepancy can be explained by variations in the labeling of tubulin dimers which, to a first approximation, can be described by a Poisson distribution, $P(m) = [\bar{m}^m/m!]\exp(-\bar{m})$, where $\bar{m}$ is the average number of fluorophores per dimer. Since $Q_m \sim m$ in Eq. (3), the amplitude of the correlation function $[G(\tau = 0) - 1]$ reduces to $(1/\bar{N})(1 + 1/\bar{m})$, $\bar{N}$ being the average number of particles. Moreover, if all of the tubulin dimers in the CrTu sample polymerize into the 8-dimer rings and the Poisson labeling distribution is preserved with $\bar{m}(\text{ring}) = 8 \times \bar{m}(\text{dimer})$, the ratio of the amplitudes of the correlation functions of the dimers to the rings will be $\kappa = (1 + 8\bar{m})/(1 + \bar{m})$. In our case, $\bar{m} \simeq 1$, which yields $\kappa = 4.5$, closer to the measured ratio (5.0).

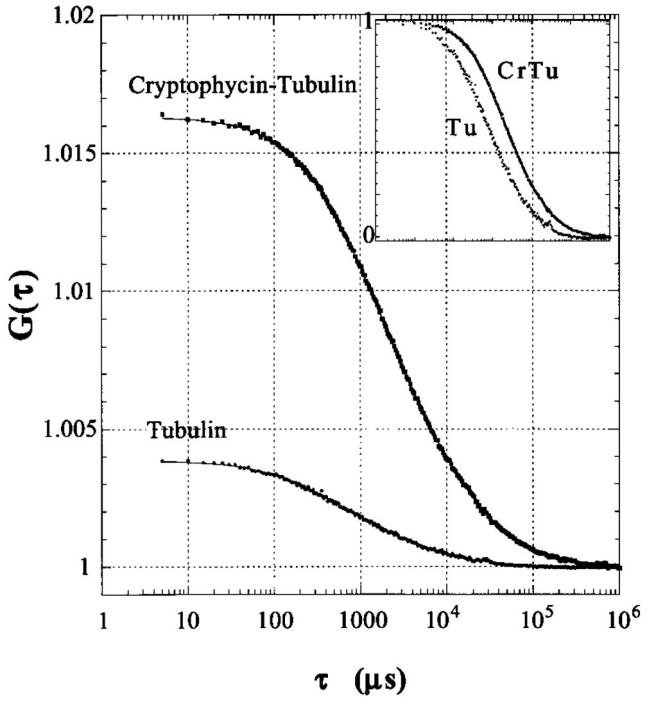

FIG. 2. Measured FCS correlation curves of tubulin and cryptophycin-tubulin samples, plotted as a function of the delay time, τ. Note the relative amplitudes of the curves as $\tau \to 0$, indicating polymerization of tubulin into rings (see text). The inset shows the same correlation curves but normalized to unity. Note the shift in characteristic time of the cyrptophycin-tubulin sample, which is another signature of polymerization.

Another signature of polymerization is evident from the inset in Fig. 2: note the time shift of the CrTu function. In Fig. 2 we include the fitting curves of the data, which were determined by nonlinear least-squares fitting of the measured correlation functions with the expression in Eq. (3) for a monodisperse system. The good fits to the data indicate a relatively narrow dispersity in size, corroborating the result already inferred from SV measurements. From these data, we determined $\tau_d(\text{Tu})/\tau_d(\text{CrTu}) = 0.364$.

An important relation linking the SV and FCS data can be derived from the ratio of the Svedberg equations of the Tu dimer and the 8-dimer rings [see Eq. (1)]:

$$\frac{s(\text{ring})}{s(\text{Tu})} = \frac{M(\text{ring})}{M(\text{Tu})}\frac{D(\text{ring})}{D(\text{Tu})} = \frac{M(\text{ring})}{M(\text{Tu})}\frac{\tau_d(\text{Tu})}{\tau_d(\text{ring})}. \quad (4)$$

In the derivation of Eq. (4) we assume the partial specific volume to be the same for both samples. Since $M(\text{ring})/M(\text{Tu}) = 8$ we obtain a simple relation that connects the ratio of the Svedberg coefficients determined from SV measurements to the ratio of the diffusion times determined independently from FCS measurements. From the FCS measurements we find $8\tau_d(\text{Tu})/\tau_d(\text{ring}) = 2.91$, in remarkable agreement with $\sigma = s(\text{ring})/s(\text{Tu}) = 2.89$ determined from SV measurements. That two measured ratios differ by less than 1% indicates their reliability, putting stringent requirements on modeling the structures of the dimers and the 8-dimer rings.

For this modeling, we wish to choose geometrical structures that can appropriately and consistently describe both the Tu dimer and the CrTu ring. We first assume the tubulin monomer to be a spherical bead with a diameter, a. In this case, tubulin is a dimer of beads and the tubulin ring is a rigid, circular, planar structure formed by 16 contiguous beads. The hydrodynamic diameter for the dimer is given by $d_{H2} = 1.437a$ [22]. For the ring, Yamakawa and Yamaki applied the modified Riseman-Kirkwood approximation and derived expressions for the components of the diffusion tensor [23]. Using their equations (Eqs. (70) and (71) in [23]) we calculate the hydrodynamic diameter of the 16-bead ring to be $d_{H16} = 4.187a$. As a result, the ratio of the hydrodynamic diameters of the dimer and the ring is $d_{H2}/d_{H16} = 0.343$, which is independent of the bead diameter. The value of this ratio differs by about 5.8% from

that of the measured ratio, $d(\mathrm{Tu})/d(\mathrm{ring}) = \tau_d(\mathrm{Tu})/\tau_d(\mathrm{ring}) = 0.364$.

This difference can be attributed to the nonspherical asymmetric shape of the tubulin monomer, captured by the 21-bead representation developed by Diaz *et al.* from small angle x-ray scattering data [8]. We apply the generic code HYDRO [24,25] to compute the corresponding hydrodynamic diameters of a dimer and a 16-monomer ring, which yields the ratio $d_{H2}/d_{H16} = 0.369$ upon setting the individual bead radii to 1.3 nm, as indicated in [8]. In contrast to the previous ratio based on spherical beads, this value is extremely close to the measured ratio (0.364), confirming that the 21-bead monomer structure is a good model for representing the tubulin monomer.

More significantly, this dimer/ring system affords a good opportunity to test the link between structure and hydrodynamic behavior of nanoscopic particles. The excellent agreement between the calculated values of the hydrodynamic radii of the dimer and the ring validates the basic hydrodynamic theory and confirms the utility of the HYDRO computational methodology. Moreover, the present results—in particular, the verification of Eq. (4)—show how suitable and complementary FCS and SV are when probing CrTu solutions. The use of ratios avoids the need for establishing experimental factors such as a full calibration of the illuminated volume of the FCS setup (for example, only p in Eq. (3) is required) and the value of the partial specific volume ($\bar{v}$) for SV.

It is worth noting that the polymerization here into closed ring structures is driven by specific attractive interactions between the CrTu complexes. In contrast, nonspecific interactions generally lead to amorphous aggregates, which are not only difficult to reproduce experimentally, but also challenging to analyze theoretically. We have demonstrated that under the studied conditions, the rings appear to be highly monodisperse, corroborating previous observations and results obtained with other techniques (cryo-electron microscopy [6] and small-angle neutron scattering [11]). In contrast to ring polymers described in the polymer science literature [26], CrTu rings are circular, appear relatively rigid, and look like toroids. Until now there has been no high-resolution experimental study of circular ring polymers because of difficulties in synthesizing appropriate samples for experimental studies [26]. By elucidating the hydrodynamic behavior of these and related tubulin rings [6,10], and by showing that the related calculations of the hydrodynamic coefficients are quantitatively correct, attention now can be given to studying the behavior of more general ring polymers having deformed circular shapes and other closed loop architectures of possible interest [26].

We acknowledge fruitful discussions with Drs. J. Douglas and J. Correia, and thank Dr. S. Mooberry for providing us with cryptophycin 1.

*Electronic address: boukarih@mail.nih.gov

[1] S. A. Allison, J. C. Herr, and J. M. Schurr, Biopolymers **20**, 469 (1981).
[2] N. V. Hud and K. H. Downing, Proc. Natl. Acad. Sci. U.S.A. **98**, 14925 (2001).
[3] J. Kuriyan and M. O'Donnell, J. Mol. Biol. **234**, 915 (1993).
[4] P. H. von Hippel and E. Delagoutee, Cell **104**, 177 (2001).
[5] A. Zhang, K. M. Wassarman, J. Ortefa, A. C. Steven and G. Storz, Mol. Cell **9**, 11 (2002).
[6] N. R. Watts, N. Cheng, W. West, A. C. Steven, and D. L. Sackett, Biochemistry **41**, 12662 (2002).
[7] E. Hamel and D. G. Covell, Curr. Med. Chem. Aniticancer Agents **2**, 19 (2002).
[8] J. F. Diaz, E. Pantos, J. Bordas, and J. M. Andreu, J. Mol. Biol. **238**, 214 (1994); J. G. de la Torre and J. M. Andreu, J. Mol. Biol. **238**, 223 (1994).
[9] J. E. Hinshaw and S. L. Schmid, Nature (London) **374**, 190 (1995).
[10] H. Boukari, R. Nossal, and D. Sackett, Biochemistry **42**, 1292 (2003).
[11] H. Boukari, V. Chernomordik, S. Krueger, R. Nossal, and D. Sackett, Physica B **350**, e533 (2004).
[12] E. L. Elson and D. Magde, Biopolymers **13**, 1 (1974); D. Magde, E. L. Elson, and W. W. Webb, Biopolymers **13**, 29 (1974).
[13] R. Aragon and S. R. Pecora, J. Chem. Phys. **64**, 1792 (1976).
[14] W. W. Webb, Appl. Opt. **40**, 3969 (2001).
[15] O. Krichevsky and G. Bonnet, Rep. Prog. Phys. **65**, 251 (2002).
[16] P. Schuck, Biophys. J. **78**, 1606 (2000); P. Schuck, M. A. Perugini, N. R. Gonzales, G. J. Howlett, and D. Schubert, Biophys. J. **82**, 1096 (2002).
[17] E. Nogales, M. Whittaker, R. A. Milligan, and K. H. Downing, Cell **96**, 79 (1999).
[18] B. Alberts, D. Bray, J. Lewis, M. Raff, K. Roberts, and J. D. Watson, *Molecular Biology of the Cell* (Garland Publishing, New York, 1994), 3rd ed..
[19] T. Svedberg and K. O. Pederson, *The Ultracentrifuge* (Oxford University Press, London, 1940).
[20] P. Schuck and B. Demeler, Biophys. J. **76**, 2288 (1999).
[21] P. Schuck, www.analyticalultracentrifugation.com/references.htm.
[22] J. B. Hubbard and J. F. Douglas, Phys. Rev. E **47**, 2983 (1993), and references therein.
[23] H. Yamakawa and J. Yamaki, J. Chem. Phys. **58**, 2049 (1973).
[24] J. G. de La Torre and V. A. Bloomfield, Q. Rev. Biophys. **14**, 81 (1981).
[25] J. G. de La Torre, S. Navarro, M. C. L. Martinez, F. G. Diaz, and J. J. L. Cascales, Biophys. J. **67**, 530 (1994).
[26] T. McLeish, Science **297**, 2005 (2002); C. W. Bielawski, D. Benitez, and R. H. Grubbs, Science **297**, 2041 (2002).